

Asymptotic Achievability of the Cramér-Rao Lower Bound of Channel Estimation for Reconfigurable Intelligent Surface Assisted Communication System

Yiming Liu, *Student Member, IEEE*, Erwu Liu, *Senior Member, IEEE*,
Rui Wang, *Senior Member, IEEE*, Binyu Lu, *Student Member, IEEE*

Abstract—To achieve the joint active and passive beamforming gains in the reconfigurable intelligent surface assisted millimeter wave system, the reflected cascade channel needs to be estimated accurately. A lot of strategies have been proposed to make such estimations. However, they cannot guarantee the achievability of the Cramér-Rao lower bound (CRLB). To solve this issue, we first convert the estimation problem into a sparse signal recovery problem by utilizing the properties of discrete Fourier matrix and Kronecker product. Then, a joint typicality estimator is utilized to carry out the signal recovery task. We show that, through both mathematical proof and numerical simulations, the proposed estimator can in fact asymptotically achieve the CRLB.

Index Terms—Reconfigurable intelligent surface, cascade channel estimation, millimeter wave, Cramér-Rao lower bound, noisy sparse signal recovery, joint typicality estimator.

I. INTRODUCTION

Reconfigurable intelligent surface (RIS), which is a meta-surface comprising of a large number of passive reflecting elements, has emerged as a promising and cost-effective solution to improve the spectrum and energy efficiency of wireless communication systems [1]–[3]. With the assistance of a smart controller, the RIS can adjust its reflection coefficients such that the desired signals are added constructively. The joint active and passive beamforming design has been studied in some existing works with continuous phase shifts (e.g., [4], [5]) or discrete phase shifts (e.g., [6], [7]) at reflecting elements. In addition, the RIS can also be introduced into a millimeter wave (mmWave) system to establish robust connections when the line-of-sight link is blocked by some obstructions [8].

It is worthy noting that, to achieve the above joint active and passive beamforming gains, the reflected cascade channel needs to be estimated accurately. Several novel strategies have been proposed to efficiently make such estimations. An on-off state control based strategy is proposed in [9] to estimate each reflected channel without interference from the other reflecting elements. To reduce the channel estimation time, [10] proposes a three-phase framework for multi-user communications. In [11], a novel hierarchical training reflection design is proposed to progressively estimate reflected channels over multiple time blocks. In [12], the orthogonal matching pursuit algorithm is utilized to estimate the cascade channel in a mmWave system.

Yiming Liu, Erwu Liu, Rui Wang, and Binyu Lu are with the College of Electronics and Information Engineering, Tongji University, Shanghai 201804, China. E-mail: ymliu_970131@tongji.edu.cn, erwu.liu@ieee.org, rui-wang@tongji.edu.cn, 2030705@tongji.edu.cn.

However, the existing strategies do not exploit the sparsity of mmWave channels which may incur many extra training overhead. Most importantly, their optimality has not been established, i.e., whether the Cramér-Rao lower bound (CRLB) of the reflected cascade channel estimation is achievable still remains uncertain. To solve this issue, we first convert the estimation problem into a noisy sparse signal recovery problem by utilizing the properties of discrete Fourier (DFT) matrix and Kronecker product. A joint typicality estimator is then utilized to carry out the recovery task and establish the asymptotic achievability of the CRLB as the product of time slot number and receive antenna number tends to infinity. This bound can be asymptotically achieved whether the estimator knows the location of the non-zero entries. To the best of our knowledge, it is the first work establishing the achievability of the CRLB of the reflected cascade channel estimation for RIS-assisted mmWave system. The validity of our result is verified through both mathematical proof and numerical simulations.

II. SYSTEM AND CHANNEL MODEL

Encouraged by the potential of mmWave and large antenna arrays in improving the spectral efficiency and data transmission quality, many standardized channel models have started to emerge [13]–[15]. We evaluate our works based on these models while introducing the RIS into the system.

A. System Model

We consider an RIS-assisted mmWave communication system, as illustrated in Fig. 1, where the BS is equipped with N_s antennas, the MS is equipped with N_d antennas, and the RIS is equipped with N_r reflecting elements. The BS and MS are placed in the horizontal plane, and the RIS is placed in the vertical plane. Although the BS and MS are equipped with a large number of antennas, they can fit within the compact form because of the small wavelength of mmWave. In addition, due to the inherent sparse scattering characteristics of mmWave channels [16], there exist only a few paths in the system. In this letter, to better illustrate our result, we neglect the line-of-sight (direct link) from the BS to the MS. Nevertheless, the extension to the scenario with direct link is straightforward. The elevation (azimuth) angle-of-departure (AoD) of the i^{th} path at the BS and RIS are denoted as θ_i (ϕ_i) and γ'_i (μ'_i), respectively. The elevation (azimuth) angle-of-arrival (AoA) of the i^{th} path at the RIS and MS are denoted as γ_i (μ_i) and ϑ_i (φ_i), respectively.

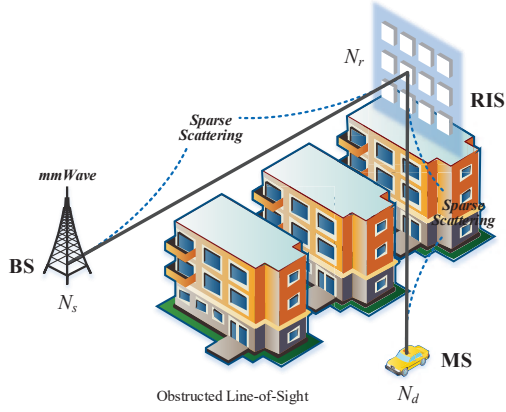


Fig. 1. The RIS-assisted mmWave communication system with an N_s -antenna BS, an N_d -antenna MS, and an RIS comprising N_r reflecting elements.

B. Channel Model

Due to the inherent sparsity of mmWave channels, the number of paths between the BS and RIS is small relative to the dimensions of BS-RIS channel matrix \mathbf{G}' , and we assume it is at most L' . Then, \mathbf{G}' can be modeled as follows:

$$\mathbf{G}' = \sqrt{\frac{N_s N_r}{\rho}} \sum_{i=1}^{L'} \alpha_i \mathbf{a}_r(\gamma_i, \mu_i) \mathbf{a}_s^H(\theta_i, \phi_i) \quad (1)$$

where ρ denotes the average path-loss between the BS and RIS, α_i is the propagation gain associated with the i^{th} path, and $\mathbf{a}_r(\gamma_i, \mu_i)$ and $\mathbf{a}_s(\theta_i, \phi_i)$ are the array response vectors at BS and RIS, respectively. We assume that the RIS deployed here is an $N_{r,h} \times N_{r,w}$ uniform planar array. Then, we have

$$\mathbf{a}_s(\theta_i, \phi_i) = [e^{j(1-1)u_s}, e^{j(2-1)u_s}, \dots, e^{j(N_s-1)u_s}]^T \quad (2)$$

$$\begin{aligned} \mathbf{a}_r(\gamma_i, \mu_i) &= \mathbf{a}_{r,h}(\gamma_i, \mu_i) \otimes \mathbf{a}_{r,w}(\gamma_i, \mu_i) \\ &= [e^{j(1-1)u_{r,h}}, e^{j(2-1)u_{r,h}}, \dots, e^{j(N_{r,h}-1)u_{r,h}}]^T \\ &\quad \otimes [e^{j(1-1)u_{r,w}}, e^{j(2-1)u_{r,w}}, \dots, e^{j(N_{r,w}-1)u_{r,w}}]^T \end{aligned} \quad (3)$$

where \otimes represents the Kronecker product, the exponential parameters: $u_s = \frac{2\pi d}{\lambda} \sin(\theta_i) \cos(\phi_i)$, $u_{r,h} = \frac{2\pi d}{\lambda} \cos(\gamma_i)$, and $u_{r,w} = \frac{2\pi d}{\lambda} \sin(\gamma_i) \cos(\mu_i)$, d is the separation between antennas (reflecting elements) at the BS (RIS), and λ is the wavelength of transmitted signal. Similarly, we assume the number of paths between the RIS and MS is at most L'' . Then, the RIS-MS channel matrix \mathbf{G}'' can be modeled as follows:

$$\mathbf{G}'' = \sqrt{\frac{N_r N_d}{\rho'}} \sum_{i=1}^{L''} \beta_i \mathbf{a}_d(\vartheta_i, \varphi_i) \mathbf{a}_r^H(\gamma'_i, \mu'_i) \quad (4)$$

where ρ' denotes the average path-loss between the RIS and user, β_i is the propagation gain associated with the i^{th} path, and $\mathbf{a}_d(\vartheta_i, \varphi_i)$ is the array response vector at the MS, which can be written as

$$\mathbf{a}_d(\vartheta_i, \varphi_i) = [e^{j(1-1)u_d}, e^{j(2-1)u_d}, \dots, e^{j(N_d-1)u_d}]^T \quad (5)$$

where $u_d = \frac{2\pi d}{\lambda} \sin(\vartheta_i) \cos(\varphi_i)$. Based on the BS-RIS and RIS-MS channel models given in Eqs. (1) and (4), the overall $N_d \times N_s$ channel matrix \mathbf{H} can be expressed as

$$\mathbf{H} = \mathbf{G}'' \Phi \mathbf{G}' \quad (6)$$

where the diagonal matrix $\Phi = \text{diag}[e^{j\varrho}]^1$ is the response at the RIS. The $N_r \times 1$ vector $\varrho = [\varrho_1, \dots, \varrho_{N_r}]^T$ represents the phase shifts of N_r reflecting elements at the RIS.

Then, the received signals $\mathbf{Y} \in \mathbb{C}^{N_d \times K}$ at the MS over K time slots can be expressed as

$$\mathbf{Y} = \mathbf{H}\mathbf{X} + \mathbf{N} \quad (7)$$

where the i^{th} column $\mathbf{x}[i]$ of \mathbf{X} is the pilot signal transmitted by the BS at the i^{th} time slot, the i^{th} column $\mathbf{n}[i]$ of \mathbf{N} is the additive white Gaussian noise at the i^{th} time slot with the elements independently drawn from $\mathcal{CN}(0, \sigma^2)$, and the transmit power at the i^{th} time slot is $p_{\text{BS}} = \mathbb{E}\{\mathbf{x}^H[i]\mathbf{x}[i]\}$.

III. SPARSE STRUCTURE OF CASCADE CHANNEL

In this section, we discuss how to convert the channel estimation problem into a noisy sparse signal recovery problem by utilizing the sparse scattering nature of mmWave channels. The channel matrices \mathbf{G}' and \mathbf{G}'' in Eqs. (1) and (4) are not visibly sparse. Thus, we express them in the angular domain as follows [17]:

$$\tilde{\mathbf{G}}' = \mathbf{U}_r^H \mathbf{G}' \mathbf{U}_s \quad (8)$$

$$\tilde{\mathbf{G}}'' = \mathbf{U}_d^H \mathbf{G}'' \mathbf{U}_r \quad (9)$$

where \mathbf{U}_s , \mathbf{U}_r and \mathbf{U}_d are the $N_s \times N_s$, $N_r \times N_r$ and $N_d \times N_d$ spartial unitary DFT matrices. By substituting Eqs. (8) and (9) into Eq. (6), we obtain that

$$\tilde{\mathbf{H}} = \mathbf{U}_d^H \mathbf{G}'' \mathbf{U}_r \Phi \mathbf{U}_r^H \mathbf{G}' \mathbf{U}_s \quad (10)$$

When the BS transmits pilot signals to the MS, the phase shifts at the RIS are set as zero, i.e., Φ is set as a unit matrix. Then, Eq. (10) can be simplified as

$$\tilde{\mathbf{H}} = \mathbf{U}_d^H \mathbf{G}'' \mathbf{G}' \mathbf{U}_s \quad (11)$$

Clearly, in Eq. (11), \mathbf{U}_s and \mathbf{U}_d act as transmit and receive beamforming matrices, respectively. A given path with parameter u_s (u_d) has almost all of its energy along one particular vector $[\mathbf{U}_s]_{:,m}$ ($[\mathbf{U}_d]_{:,n}$), if m (n) satisfies: [17]

$$\left| u_s - \frac{2\pi(m-1)}{N_s} \right| < \frac{2\pi}{N_s}, \quad (12)$$

$$\left| u_d - \frac{2\pi(n-1)}{N_d} \right| < \frac{2\pi}{N_d}. \quad (13)$$

In order to illustrate visually, Fig. 2 plots a specific realization for the channel magnitude in the angular domain. As seen from it, the true channel is indeed sparse in the angular domain, i.e., it exhibits a few dominant coefficients. As a result, the RIS-assisted mmWave channel is inherently sparse in the angular domain if expressed in suitable DFT bases. Using the DFT precoder \mathbf{U}_s and combiner \mathbf{U}_d^H in Eq. (11) and vectorizing the received signals at the MS yields

$$\begin{aligned} \mathbf{y} &= \text{vec}(\tilde{\mathbf{H}}\mathbf{X}) + \text{vec}(\mathbf{U}_d^H \mathbf{N}) \\ &= (\mathbf{X}^T \otimes \mathbf{I}_{N_d}) \text{vec}(\tilde{\mathbf{H}}) + \text{vec}(\mathbf{U}_d^H \mathbf{N}) \\ &= \Upsilon \mathbf{v} + \mathbf{n} \end{aligned} \quad (14)$$

¹Since the RIS is a passive device, each reflecting element is usually designed to maximize the signal reflection. Thus, we set the amplitude of reflection coefficient equal to one for simplicity in this letter.

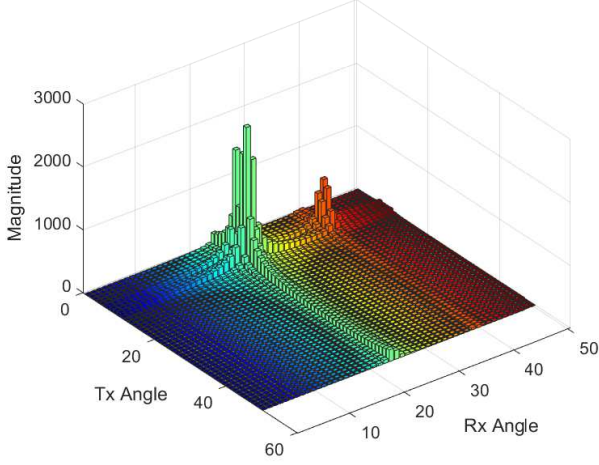


Fig. 2. Angular-domain channel for $N_s = 50$, $N_d = 50$, and $N_r = 40$. BS-RIS channel has 2 paths and RIS-MS channel has 2 paths.

where $\mathbf{Y} = \mathbf{X}^T \otimes \mathbf{I}_{N_d}$ is the $KN_d \times N_s N_d$ measurement matrix, $\mathbf{v} = \text{vec}(\hat{\mathbf{H}})$ is the $N_s N_d \times 1$ sparse signal we need to recovery, and \mathbf{n} is the additive white Gaussian noise. We assume that \mathbf{v} is sparse with at most $L \propto L' * L''$ nonzero coefficients in unknown locations. Once \mathbf{v} is recovered, an estimate of the original channel matrix $\hat{\mathbf{H}}$ is readily obtained as follows:

$$\hat{\mathbf{H}} = \mathbf{U}_d \hat{\mathbf{H}} \mathbf{U}_s^H \quad (15)$$

where $\hat{\mathbf{H}} = \text{unvec}(\hat{\mathbf{v}})$ and $\hat{\mathbf{v}}$ is an estimate of \mathbf{v} .

Now, we have converted the channel estimation problem into a noisy sparse signal recovery problem in Eq. (14).

IV. ASYMPTOTIC ACHIEVABILITY OF THE CRAMÉR-RAO LOWER BOUND VIA JOINT TYPICALITY ESTIMATOR

Many classical compressed sensing algorithms such as basis pursuit (BP) [18] and orthogonal matching pursuit (OMP) [19] can be utilized to recover the sparse signal \mathbf{v} . However, these algorithms always choose the locally optimal approximation to the actual sparse signal [18]–[22]. Thus, in this section, we utilize Shannon theory and the notion of joint typicality [23], [24] to asymptotically achieve the CRLB of the channel estimation for RIS-assisted mmWave system where the estimator have no knowledge of the locations of the nonzero entries in \mathbf{v} . To prove the asymptotic achievability of the CRLB, we first state the following lemmas:

Lemma 1. *Let the set $\mathcal{J} \subset \{1, \dots, N_s N_d\}$ such that $|\mathcal{J}| = L$ and $\mathbf{Y}_{\mathcal{J}}$ be the sub-matrix of the measurement matrix \mathbf{Y} with the columns corresponding to the index set \mathcal{J} . Then, we have $\text{rank}(\mathbf{Y}_{\mathcal{J}}) = L$ with probability 1.*

Proof: First, we consider the rank of \mathbf{X}^T . The $(m, n)^{\text{th}}$ entry of it represents the pilot symbol transmitted by the n^{th} antenna at the m^{th} time slot. Thus, all of the entries in it are independent and designable. For simplicity, we set them as independent and identically distributed (i.i.d.) and distributed

according to $\mathcal{CN}(0, 1)$. Let \mathbf{x}_i and \mathbf{x}_j be two columns of \mathbf{X}^T . Utilizing the law of large numbers yields:

$$\mathbf{x}_i^H \mathbf{x}_j = \sum_k x_{k,i}^* x_{k,j} \rightarrow 0, \quad i \neq j \quad (16)$$

as K goes to infinity. Thus, the columns of \mathbf{X}^T are mutually orthogonal with probability 1, i.e., \mathbf{X}^T is a full column rank matrix when $K > N_s$. Then, due to \mathbf{I}_{N_d} is a unit matrix, it has a full column rank. By utilizing the rank property of the Kronecker product: $\text{rank}(\mathbf{Y}) = \text{rank}(\mathbf{X}^T) \text{rank}(\mathbf{I}_{N_d})$, we prove the statement of the Lemma. ■

Definition 1. (δ -Jointly Typicality)

The received signal \mathbf{y} collected over K time slots, and the set of indices $\mathcal{J} \subset \{1, 2, \dots, N_s N_d\}$ with $|\mathcal{J}| = L$ are δ -joint typical, if $\text{rank}(\mathbf{Y}_{\mathcal{J}}) = L$ and

$$\left| \frac{1}{KN_d} \|\mathbf{\Pi}_{\mathbf{Y}_{\mathcal{J}}}^{\perp} \mathbf{y}\|^2 - \frac{KN_d - L}{KN_d} \sigma^2 \right| < \delta \quad (17)$$

where $\mathbf{Y}_{\mathcal{J}}$ is the sub-matrix of the measurement matrix \mathbf{Y} with the columns corresponding to the index set \mathcal{J} , and $\mathbf{\Pi}_{\mathbf{Y}_{\mathcal{J}}}^{\perp} = \mathbf{I} - \mathbf{Y}_{\mathcal{J}}(\mathbf{Y}_{\mathcal{J}}^H \mathbf{Y}_{\mathcal{J}})^{-1} \mathbf{Y}_{\mathcal{J}}^H$ is the orthogonal projection matrix.

Theorem 1. *The Joint Typicality Estimator [24], [25] can be utilized to estimate the channel in an RIS-assisted mmWave system, i.e., solve the sparse signal recovery problem in Eq. (14). The detailed steps are illustrated in Algorithm 1.*

Proof: Based on Lemma 1 and Definition 1, the measurement matrix \mathbf{Y} in Eq. (14) has been proved to be full column rank, which ensures that the subspaces spanned by different L column vectors chosen from the matrix \mathbf{Y} are different. If L column vectors are chosen correctly, there exists only additive white Gaussian noise in the orthogonal complement. Thus, the joint typicality estimator can be utilized to solve the noisy sparse signal recovery problem in Eq. (14). ■

In order to further prove that we can asymptotically achieve the CRLB on the estimation error where the estimator have no knowledge of the locations of the nonzero entries of \mathbf{v} , we state the following lemmas:

Lemma 2. *For any unbiased estimate $\hat{\mathbf{v}}$ of \mathbf{v} , the Cramér-Rao lower bound on the MSE is given as*

$$\mathbb{E} \{ \|\hat{\mathbf{v}} - \mathbf{v}\|^2 \} \geq \sigma^2 \text{Tr} [(\mathbf{Y}_{\mathcal{I}}^H \mathbf{Y}_{\mathcal{I}})^{-1}]. \quad (18)$$

Proof: The likelihood function of the random vector \mathbf{y} conditioned on \mathbf{v} is

$$p(\mathbf{y}; \mathbf{v}) = \frac{\exp(-\frac{1}{2\sigma^2} \|\mathbf{y} - \mathbf{Y}_{\mathcal{I}} \mathbf{v}_{\mathcal{I}}\|^2)}{(2\pi)^{KN_d/2} \sigma^{KN_d}} \quad (19)$$

where $\mathbf{v}_{\mathcal{I}}$ is the subvector of \mathbf{v} with elements corresponding to the index set \mathcal{I} . Then, by using Eq. (6) in [26], the CRLB can be written as Eq. (18). ■

Lemma 3. (Lemma 2.3 of [27])

Let $\mathcal{I} = \text{supp}(\mathbf{v})$ and $\text{rank}(\mathbf{Y}_{\mathcal{I}}) = L$. Then, for $\delta > 0$, it

Algorithm 1 Joint Typicality Based Channel Estimator

- 1: **Input:** The numbers of antennas N_s at the BS and N_d at the MS, the pilot signal \mathbf{X} , the received signal vector \mathbf{y} , and the maximal sparse-level L .
- 2: **while** the index set \mathcal{J}_{i-1} is not δ -jointly typical with \mathbf{y} **do**
- 3: i^{th} iteration of all the possible $\binom{N_s N_d}{L}$ L -dimensional subspaces :
- 4: Determine whether the following inequality is satisfied.

$$\left| \frac{1}{KN_d} \|\mathbf{\Pi}_{\mathbf{Y}_{\mathcal{J}_i}}^\perp \mathbf{y}\|^2 - \frac{KN_d - L}{KN_d} \sigma^2 \right| < \delta$$

- 5: If it is satisfied, compute the estimate $\hat{\mathbf{v}}$ by projecting the received signal \mathbf{y} onto the subspace spanned by $\mathbf{Y}_{\mathcal{J}_i}$.

$$\hat{\mathbf{v}} = (\mathbf{Y}_{\mathcal{J}}^H \mathbf{Y}_{\mathcal{J}})^{-1} \mathbf{Y}_{\mathcal{J}}^H \mathbf{y}$$

- 6: If there exists no set that is δ -typical to \mathbf{y} , it outputs the zero vector.
 - 7: **end while**
 - 8: **Output:** The channel estimate $\hat{\mathbf{H}} = \mathbf{U}_d \text{unvec}(\hat{\mathbf{v}}) \mathbf{U}_s^H$.
-

holds that

$$\begin{aligned} & \mathbb{P} \left(\left| \frac{1}{KN_d} \|\mathbf{\Pi}_{\mathbf{Y}_{\mathcal{J}}}^\perp \mathbf{y}\|^2 - \frac{KN_d - L}{KN_d} \sigma^2 \right| > \delta \right) \\ & \leq 2 \exp \left(-\frac{\delta^2}{4\sigma^4} \frac{K^2 N_d^2}{KN_d - L + \frac{2\delta}{\sigma^2} KN_d} \right). \end{aligned} \quad (20)$$

Let \mathcal{J} be an index set such that $|\mathcal{J}| = L$, $|\mathcal{I} \cap \mathcal{J}| < L$, and $\text{rank}(\mathbf{Y}_{\mathcal{J}}) = L$. Then, for $\delta > 0$, it holds that

$$\begin{aligned} & \mathbb{P} \left(\left| \frac{1}{KN_d} \|\mathbf{\Pi}_{\mathbf{Y}_{\mathcal{J}}}^\perp \mathbf{y}\|^2 - \frac{KN_d - L}{KN_d} \sigma^2 \right| < \delta \right) \\ & \leq \exp \left(\frac{L - KN_d}{4} \left(\frac{\sum_{k \in \mathcal{I} \setminus \mathcal{J}} |v_k|^2 - \delta'}{\sum_{k \in \mathcal{I} \setminus \mathcal{J}} |v_k|^2 + \sigma^2} \right)^2 \right) \end{aligned} \quad (21)$$

where v_k is the k^{th} entry in \mathbf{v} and

$$\delta' = \delta \frac{KN_d}{KN_d - L}. \quad (22)$$

Proof: Please refer to [27] for the proof. \blacksquare

Theorem 2. By utilizing the Joint Typicality based channel estimator given in Algorithm 1, the MSE of cascade channel estimation in an RIS-assisted mmWave system asymptotically achieves the Cramér-Rao lower bound as the product of time slot number and receive antenna number tends to infinity. This bound can be asymptotically achieved whether the estimator know the location of the non-zero entries.

Proof: The MSE of the joint typicality estimator (averaged over all possible measurement matrices) can be upper-bounded as follows:

$$\begin{aligned} \varepsilon_\delta(KN_d) &= \mathbb{E} \{ \|\hat{\mathbf{v}} - \mathbf{v}\|^2 \} \\ &\leq \int_{\mathbf{Y}} \|\mathbf{v}\|^2 \mathbb{P}(E_0) dP(\mathbf{Y}) \\ &\quad + \int_{\mathbf{Y}} \mathbb{E}_{\mathbf{n}|\mathbf{Y}} \{ \|\mathbf{Y}_{\mathcal{I}}^H \mathbf{Y}_{\mathcal{I}}^{-1} \mathbf{Y}_{\mathcal{I}}^H \mathbf{y} - \mathbf{v}\|^2 \} \\ &\quad \times \mathbb{P}(\mathcal{I} \sim \mathbf{y}) dP(\mathbf{Y}) \\ &\quad + \int_{\mathbf{Y}} \sum_{\mathcal{J} \neq \mathcal{I}} \mathbb{E}_{\mathbf{n}|\mathbf{Y}} \{ \|\mathbf{Y}_{\mathcal{J}}^H \mathbf{Y}_{\mathcal{J}}^{-1} \mathbf{Y}_{\mathcal{J}}^H \mathbf{y} - \mathbf{v}\|^2 \} \\ &\quad \times \mathbb{P}(\mathcal{J} \sim \mathbf{y}) dP(\mathbf{Y}) \end{aligned} \quad (23)$$

where $\mathbb{P}(\cdot)$ represents the event probability defined over the noise density, the event E_0 represents the estimator does not find any set δ -typical to \mathbf{y} , $dP(\mathbf{Y})$ represents the probability measure of the matrix \mathbf{Y} , and the inequality follows from the Boole's inequality. The second term is corresponding to \mathcal{I} and is the MSE of a genie-aided estimation where the estimator knows $\text{supp}(\mathbf{v})$. We rewritten it as follows:

$$\begin{aligned} & \int_{\mathbf{Y}} \mathbb{E}_{\mathbf{n}|\mathbf{Y}} \{ \|\mathbf{Y}_{\mathcal{I}}^H \mathbf{Y}_{\mathcal{I}}^{-1} \mathbf{Y}_{\mathcal{I}}^H \mathbf{y} - \mathbf{v}\|^2 \} \mathbb{P}(\mathcal{I} \sim \mathbf{y}) dP(\mathbf{Y}) \\ &= \mathbb{E}_{\mathbf{n}, \mathbf{Y}} \{ \|\mathbf{Y}_{\mathcal{I}}^H \mathbf{Y}_{\mathcal{I}}^{-1} \mathbf{Y}_{\mathcal{I}}^H \mathbf{n}\|^2 \} = \mathbb{E}_{\mathbf{Y}} \{ \sigma^2 \text{Tr}(\mathbf{Y}_{\mathcal{I}}^H \mathbf{Y}_{\mathcal{I}})^{-1} \}. \end{aligned} \quad (24)$$

By using Lemma 2, we obtain that the second term in Eq. (23) is the CRLB of the genie-aided cascade channel estimation.

Next, we show that the first and second term in Eq. (23) converge to zero when $KN_d \rightarrow \infty$. By using Lemma 3, the first term can be upper-bounded as

$$\begin{aligned} & \int_{\mathbf{Y}} \|\mathbf{v}\|^2 \mathbb{P}(E_0) dP(\mathbf{Y}) \\ & \leq 2 \|\mathbf{v}\|^2 \exp \left(-\frac{\delta^2}{4\sigma^4} \frac{K^2 N_d^2}{KN_d - L + \frac{2\delta}{\sigma^2} KN_d} \right). \end{aligned} \quad (25)$$

This term approaches to zero as $KN_d \rightarrow \infty$, since $\|\mathbf{v}\|^2$ does not grows and the exponential term tends to negative infinity as $KN_d \rightarrow \infty$. By using Lemma 3, the third term can be upper-bounded as

$$\begin{aligned} & \int_{\mathbf{Y}} \sum_{\mathcal{J} \neq \mathcal{I}} \mathbb{E}_{\mathbf{n}|\mathbf{Y}} \{ \|\mathbf{Y}_{\mathcal{J}}^H \mathbf{Y}_{\mathcal{J}}^{-1} \mathbf{Y}_{\mathcal{J}}^H \mathbf{y} - \mathbf{v}\|^2 \} \\ & \quad \times \mathbb{P}(\mathcal{J} \sim \mathbf{y}) dP(\mathbf{Y}) \\ & \leq (L\sigma^2 + \|\mathbf{v}\|^2) \int_{\mathbf{Y}} \sum_{\mathcal{J} \neq \mathcal{I}} \mathbb{E}_{\mathbf{n}|\mathbf{Y}} \mathbb{P}(\mathcal{J} \sim \mathbf{y}) dP(\mathbf{Y}) \\ & \leq (L\sigma^2 + \|\mathbf{v}\|^2) \times \\ & \quad \sum_{\mathcal{J} \neq \mathcal{I}} \exp \left(\frac{L - KN_d}{4} \left(\frac{\sum_{k \in \mathcal{I} \setminus \mathcal{J}} |v_k|^2 - \delta'}{\sum_{k \in \mathcal{I} \setminus \mathcal{J}} |v_k|^2 + \sigma^2} \right)^2 \right). \end{aligned} \quad (26)$$

This term tends to zero as $KN_d \rightarrow \infty$, since $(L\sigma^2 + \|\mathbf{v}\|^2)$ does not grows and $(L - KN_d)$ tends to negative infinity as $KN_d \rightarrow \infty$. \blacksquare

V. NUMERICAL RESULTS

In this section, we numerically illustrate the result given in Theorem 2. To verify whether the CRLB of cascade channel estimation for RIS-assisted mmWave communication system can be asymptotically achieved when the product of time slot number and receive antenna number KN_d tends to infinity, Fig. 3 simultaneously plots the curves of the CRLB, the MSE upper bound, and the performance of joint typicality estimator versus the time slot number K with different signal-to-noise ratios (SNRs) in the set of $\{20 \text{ dB}, 30 \text{ dB}, 40 \text{ dB}\}$. In this figure, the numbers of antennas at the BS and MS are both set as 5, and the number of reflecting elements at the RIS is set as 10. The path numbers in the BS-RIS channel and the RIS-MS channel are both set as 1. In addition, the numerical results in Fig. 3 are obtained through 1000 Monte Carlo trials. It is observed that the CRLB can be achieved as the time slot number tends to infinity, which confirms the results in Theorem 2. When we fix the time slot number K and change receive antenna number N_d , the curves are similar to Fig. 3.

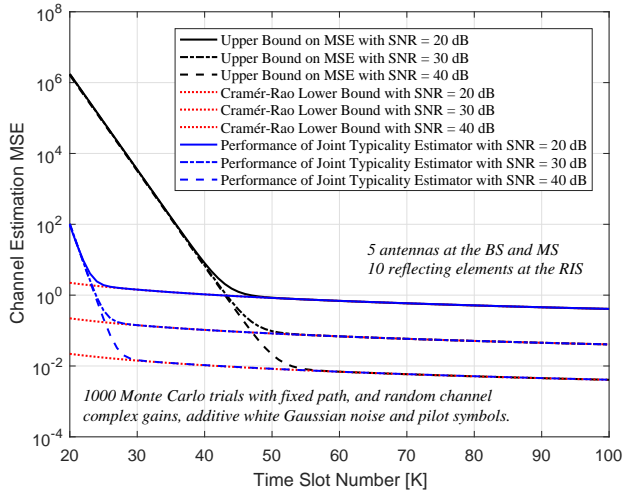


Fig. 3. The performance of joint typicality based channel estimator versus the time slot number with different SNRs.

VI. CONCLUSION

In this letter, we consider the reflected cascade channel estimation in an RIS-assisted mmWave communication system. By utilizing the joint typicality based channel estimator, the MSE of estimation can asymptotically achieve the CRLB as the number of time slots or that of receive antennas tends to infinity. This bound can be asymptotically achieved whether the estimator knows the location of the non-zero entries. To the best of our knowledge, it is the first work which establishes the asymptotic achievability of the CRLB of the reflected cascade channel estimation for the RIS-assisted mmWave communication systems.

REFERENCES

[1] Ö. Özdoğan, E. Björnson, and E. G. Larsson, “Intelligent reflecting surfaces: Physics, propagation, and pathloss modeling,” *IEEE Wireless Communications Letters*, vol. 9, no. 5, pp. 581–585, 2020.

[2] C. Huang, A. Zappone, G. C. Alexandropoulos, M. Debbah, and C. Yuen, “Reconfigurable intelligent surfaces for energy efficiency in wireless communication,” *IEEE Transactions on Wireless Communications*, vol. 18, no. 8, pp. 4157–4170, 2019.

[3] Y. Liu, E. Liu, and R. Wang, “Energy efficiency analysis of intelligent reflecting surface system with hardware impairments,” in *2020 IEEE Global Communications Conference (GLOBECOM 2020)*, Taipei, Taiwan, December 2020.

[4] Q. Wu and R. Zhang, “Intelligent reflecting surface enhanced wireless network via joint active and passive beamforming,” *IEEE Transactions on Wireless Communications*, vol. 18, no. 11, pp. 5394–5409, 2019.

[5] S. Lin, B. Zheng, G. C. Alexandropoulos, M. Wen, F. Chen, and S. Mumtaz, “Adaptive transmission for reconfigurable intelligent surface-assisted ofdm wireless communications,” *IEEE Journal on Selected Areas in Communications*, vol. 38, no. 11, pp. 2653–2665, 2020.

[6] Q. Wu and R. Zhang, “Beamforming optimization for wireless network aided by intelligent reflecting surface with discrete phase shifts,” *IEEE Transactions on Communications*, vol. 68, no. 3, pp. 1838–1851, 2020.

[7] H. Guo, Y. C. Liang, J. Chen, and E. G. Larsson, “Weighted sum-rate maximization for intelligent reflecting surface enhanced wireless networks,” in *2019 IEEE Global Communications Conference (GLOBECOM)*, 2019, pp. 1–6.

[8] X. Tan, Z. Sun, D. Koutsonikolas, and J. M. Jornet, “Enabling indoor mobile millimeter-wave networks based on smart reflect-arrays,” in *IEEE INFOCOM 2018 - IEEE Conference on Computer Communications*, 2018, pp. 270–278.

[9] Y. Yang, B. Zheng, S. Zhang, and R. Zhang, “Intelligent reflecting surface meets OFDM: Protocol design and rate maximization,” *IEEE Transactions on Communications*, vol. 68, no. 7, pp. 4522–4535, 2020.

[10] Z. Wang, L. Liu, and S. Cui, “Channel estimation for intelligent reflecting surface assisted multiuser communications: Framework, algorithms, and analysis,” *IEEE Transactions on Wireless Communications*, vol. 19, no. 10, pp. 6607–6620, 2020.

[11] C. You, B. Zheng, and R. Zhang, “Channel estimation and passive beamforming for intelligent reflecting surface: Discrete phase shift and progressive refinement,” *IEEE Journal on Selected Areas in Communications*, vol. 38, no. 11, pp. 2604–2620, 2020.

[12] P. Wang, J. Fang, H. Duan, and H. Li, “Compressed channel estimation for intelligent reflecting surface-assisted millimeter wave systems,” *IEEE Signal Processing Letters*, vol. 27, pp. 905–909, 2020.

[13] A. Shahmansoori, G. E. Garcia, G. Destino, G. Seco-Granados, and H. Wymeersch, “Position and orientation estimation through millimeter-wave MIMO in 5G systems,” *IEEE Transactions on Wireless Communications*, vol. 17, no. 3, pp. 1822–1835, 2018.

[14] Q. Nadeem, A. Kammoun, M. Debbah, and M. Alouini, “3D massive MIMO systems: Modeling and performance analysis,” *IEEE Transactions on Wireless Communications*, vol. 14, no. 12, pp. 6926–6939, 2015.

[15] B. Zhou, A. Liu, and V. Lau, “Successive localization and beamforming in 5G mmWave MIMO communication systems,” *IEEE Transactions on Signal Processing*, vol. 67, no. 6, pp. 1620–1635, 2019.

[16] M. R. Akdeniz, Y. Liu, M. K. Samimi, S. Sun, S. Rangan, T. S. Rappaport, and E. Erkip, “Millimeter wave channel modeling and cellular capacity evaluation,” *IEEE Journal on Selected Areas in Communications*, vol. 32, no. 6, pp. 1164–1179, 2014.

[17] F. Bellili, F. Sotgiu, and W. Yu, “Generalized approximate message passing for massive mimo mmwave channel estimation with laplacian prior,” *IEEE Transactions on Communications*, vol. 67, no. 5, pp. 3205–3219, 2019.

[18] D. L. Donoho, “Compressed sensing,” *IEEE Transactions on Information Theory*, vol. 52, no. 4, pp. 1289–1306, 2006.

[19] J. A. Tropp and A. C. Gilbert, “Signal recovery from random measurements via orthogonal matching pursuit,” *IEEE Transactions on Information Theory*, vol. 53, no. 12, pp. 4655–4666, 2007.

[20] M. A. Davenport and M. B. Wakin, “Analysis of orthogonal matching pursuit using the restricted isometry property,” *IEEE Transactions on Information Theory*, vol. 56, no. 9, pp. 4395–4401, 2010.

[21] D. Needell and R. Vershynin, “Signal recovery from incomplete and inaccurate measurements via regularized orthogonal matching pursuit,” *IEEE Journal of Selected Topics in Signal Processing*, vol. 4, no. 2, pp. 310–316, 2010.

[22] W. Dai and O. Milenkovic, “Subspace pursuit for compressive sensing signal reconstruction,” *IEEE Transactions on Information Theory*, vol. 55, no. 5, pp. 2230–2249, 2009.

[23] T. M. Cover and J. M. Thomas, *Elements of Information Theory*. New York: Wiley, 2006.

- [24] B. Babadi, N. Kalouptsidis, and V. Tarokh, "Asymptotic achievability of the Cramér–Rao Bound for noisy compressive sampling," *IEEE Transactions on Signal Processing*, vol. 57, no. 3, pp. 1233–1236, 2009.
- [25] R. Niazadeh, M. Babaie-Zadeh, and C. Jutten, "On the achievability of Cramér–Rao Bound in noisy compressed sensing," *IEEE Transactions on Signal Processing*, vol. 60, no. 1, pp. 518–526, 2012.
- [26] S. L. Collier, "Fisher information for a complex Gaussian random variable: Beamforming applications for wave propagation in a random medium," *IEEE Transactions on Signal Processing*, vol. 53, no. 11, pp. 4236–4248, 2005.
- [27] M. Akcakaya and V. Tarokh, "Shannon-theoretic limits on noisy compressive sampling," *IEEE Transactions on Information Theory*, vol. 56, no. 1, pp. 492–504, 2010.